

Condensation of $[\text{Si}_3\text{O}_9]^{6-}$ Anions in the Solid State to the Dimeric Cyclotrisilicate Anion $[\text{Si}_6\text{O}_{17}]^{10-}$

Stefan Hoffmann[‡] and Thomas F. Fässler^{*†}

Department Chemie, Technische Universität München, Lichtenbergstrasse 4, D-85747 Garching, Germany, and Max-Planck-Institut für Chemische Physik fester Stoffe, Nöthnitzer Str. 40, 01187 Dresden, Germany

Received June 16, 2006

The structure of the silicate $\text{Rb}_{10}[\text{Si}_6\text{O}_{17}]$ containing a novel dimeric cyclotrisilicate anion is reported. The compound is formed by the reaction of a mixture of SiO_2 and Rb at temperatures above 700 °C. Systematic investigations by means of differential thermal analysis and temperature-dependent powder X-ray diffraction experiments revealed that the new compound evolved from $\text{Rb}_6[\text{Si}_3\text{O}_9]$, which occurred as an intermediate product. Thus, the dimeric anion $[\text{Si}_6\text{O}_{17}]^{10-}$ is formed by condensation of the monomeric cyclotrisilicate $[\text{Si}_3\text{O}_9]^{6-}$. For both silicates, $[\text{Si}_6\text{O}_{17}]^{10-}$ and $[\text{Si}_3\text{O}_9]^{6-}$, the characteristic ring vibration modes were observed in the IR spectrum. The structure of $\text{Rb}_{10}[\text{Si}_6\text{O}_{17}]$ was solved and refined from single-crystal X-ray diffraction data in the orthorhombic space group *Pbca* (No. 61). Synthesis and structure determination of $\text{Rb}_{10}[\text{Si}_6\text{O}_{17}]$ bridge the gap to show that the recently reported structures of $\text{Rb}_{14}[\text{Si}_4][\text{Si}_6\text{O}_{17}]$ and $\text{Rb}_{14}[\text{Ge}_4][\text{Si}_6\text{O}_{17}]$ are indeed fascinating intergrowth structures of the stable oxide $\text{Rb}_{10}[\text{Si}_6\text{O}_{17}]$ and the Zintl phases RbSi (Rb_4Si_4) and RbGe (Rb_4Ge_4), respectively.

Introduction

The fascinating structural chemistry of silicates is caused by the fact that despite the simple building block $[\text{SiO}_4]$ a huge variety of structures can be observed depending on the cations employed for compensation of the negative charge of the silicate anions.¹ The structural motifs obtained by condensation reactions range from simple dimeric units $[\text{Si}_2\text{O}_7]^{6-}$, one-dimensional linear chains, two-dimensional sheets, and other infinite two- and three-dimensional structures and include also a large number of isolated ring structures. The smallest unbranched ring consisting of three condensed $[\text{SiO}_4]$ tetrahedra is found in the mineral benitoite $\text{BaTi}[\text{Si}_3\text{O}_9]$.¹ The general formula for the family of ring silicates can be written as $[\text{Si}_n\text{O}_{3n}]^{2n-}$, with reported solid-state structures for $n = 3, 4, 6, 8, 9, 12,$ and 18 .^{1,2} Furthermore, trimethylsilylestere with $n = 7^3$ and 10^1 have

been isolated, and ²⁹Si NMR experiments have revealed the presence of many other representatives in alkaline silica solutions.⁴

So far, only four structurally characterized rubidium silicates have been reported: the group silicate $\text{Rb}_6[\text{Si}_2\text{O}_7]$,^{5,6} the cyclotrisilicate $\text{Rb}_6[\text{Si}_3\text{O}_9]$,^{6,7} and the phyllosilicates (layered silicate) $\text{Rb}_2[\text{Si}_2\text{O}_5]$ ⁸ and $\text{Rb}_6[\text{Si}_{10}\text{O}_{23}]$.⁹ A systematic investigation of the phase diagram of Rb–Si–O in the range Rb_2SiO_3 – SiO_2 was published in 1963, mentioning three crystalline rubidium silicates.¹⁰

During our extensive studies of Zintl phases, we have recently discovered a new type of compound with the formula $\text{Rb}_{14}[\text{E}_4][\text{Si}_6\text{O}_{17}]$ ($\text{E} = \text{Si}$ and Ge),¹¹ which can be described as “double salts” containing both Zintl-type and silicate anions. Apart from the fact that these compounds embody two group 14 elements with a remarkable difference

* Author to whom correspondence should be addressed. E-mail: thomas.faessler@lrz.tum.de.

[†] Technische Universität München.

[‡] Max-Planck-Institut für Chemische Physik fester Stoffe.

- (1) Liebau, F. *Structural chemistry of silicates*; Springer-Verlag: Berlin, 1985.
- (2) Yamnova, N. A.; Rastscvetava, R. K.; Puscharovskii, D. Y.; Mernaf, T.; Mikheeva, M.; Khomyakov, A. P. *Kristallografiya* **1992**, *37*, 334–344.
- (3) Smolin, Y. I.; Shepelev, Y. F.; Ershov, A. S.; Hoebbel, D. Z. *Kristallogr.* **1993**, *203*, 73–78.

- (4) Knight, C. T. G. *J. Chem. Soc., Dalton Trans.* **1988**, *6*, 1457–1460.
- (5) Schartau, W.; Hoppe, R. *Naturwissenschaften* **1973**, *60*, 256.
- (6) Hoch, C.; Röhr, C. *Z. Naturforsch., B: Chem. Sci.* **2001**, *56*, 423–430.
- (7) Werthmann, R.; Hoppe, R. *Rev. Chim. Min.* **1981**, *18*, 593–607.
- (8) de Jong, B. H. W. S.; Slaats, P. G. G.; Supèr, H. T. J.; Veldman, N.; Spek, A. L. *J. Non-Cryst. Solids* **1994**, *176*, 164–171.
- (9) Schichl, H.; Völlenkle, H.; Wittmann, A. *Monatsh. Chem.* **1973**, *104*, 854–863.
- (10) Alekseeva, Z. D. *Russ. J. Inorg. Chem.* **1963**, *8*, 741–744.
- (11) Hoffmann, S.; Fässler, T. F.; Hoch, C.; Röhr, C. *Angew. Chem.* **2001**, *113*, 4527–4529.

of five in their formal oxidation number at the same time (E(−I) in $[\text{E}_4]^{4-}$ and E(IV) in $[\text{Si}_6\text{O}_{17}]^{10-}$), they also contain the so far unknown dimeric cyclotrisilicate anion $[\text{Si}_6\text{O}_{17}]^{10-}$.

Herein, we report the synthesis and single-crystal X-ray structure determination of a new rubidium silicate with the same anion, $\text{Rb}_{10}[\text{Si}_6\text{O}_{17}]$, and present experimental studies which should shed some light on the mechanism of its formation. Furthermore the IR spectroscopic data of the compounds $\text{Rb}_6[\text{Si}_3\text{O}_9]$ and $\text{Rb}_{10}[\text{Si}_6\text{O}_{17}]$ are reported.

Experiments

Synthesis. Single crystals of $\text{Rb}_{10}[\text{Si}_6\text{O}_{17}]$ have been obtained for the first time by accident from the reaction of rubidium, quartz, and germanium in the molar ratio 7:3:2 (overall sample weight: 500 mg). The educts were heated in a sealed niobium ampule to 700 °C, with a heating rate of 90 K/h, followed by an equilibration time of 24 h and a cooling ramp with the same rate. The product was isolated in small amounts as transparent moisture-sensitive red crystals.

The systematic high-yield synthesis could be achieved by reacting rubidium with crystalline quartz at a molar ratio of 5:3 (overall sample weight: 500 mg) in sealed niobium ampules at 400, 500, 600, 700, and 800 °C. The ampules were heated at 1 K/min to the final temperature. After an equilibration time of 24 h, the samples were cooled at the same rate, and the products were examined by X-ray powder diffraction analysis (STOE, STADIP II, Ge monochromator, $\text{Cu K}\alpha_1$ radiation). Excessive rubidium, indicated by a silvery appearance of the product, was removed by a subsequent sublimation in a vacuum. After the removal of rubidium, the product obtained by the reaction at 600 °C was subsequently examined by differential thermal analysis (Netzsch, DSC 404) in a closed Nb crucible (200 mg), by IR spectroscopy (NICOLET Impact 400, KBr Uvasol Merck KGaA) and by high-temperature X-ray powder diffraction analysis (graphite oven, STOE). In the latter case, the sample was filled into an open quartz capillary ($d = 0.3$ mm, Hilgenberg), which was located inside a glue-sealed quartz capillary 0.5 mm in diameter. Finally, the red crystals were investigated by continuous-wave electron paramagnetic resonance (CW-EPR) spectroscopy at ambient and liquid-nitrogen temperatures, using a Bruker ESP 300E spectrometer.

Structure Determination. A red transparent crystal was mounted in a glass capillary, which was sealed afterward (crystal dimensions $0.2 \times 0.1 \times 0.05$, trapezoid platelet). Data were collected at 150 K (Oxford Cryosystems, Cryostream Controller 700) on a two-circle STOE IPDS II diffractometer equipped with a graphite monochromator (Mo $\text{K}\alpha$ radiation, $\lambda = 0.71073$ Å) and an image plate detector at a 100 mm distance from the crystal. Images were taken for $\phi_1 = 0^\circ$ and $\varpi_1 = 0-180^\circ$ and $\phi_2 = 90^\circ$ and $\varpi_2 = 0-180^\circ$ with $\Delta\varpi = 1^\circ$ and a 2 min exposure time. A numerical absorption correction was carried out with the programs X-Shape and X-RED.¹² The structure was solved with the program package WinGX¹³ by direct methods, followed by difference Fourier methods in the space group *Pbca* (No. 61). Further details on the data collection and refinement procedure are given in Table 1. The fractional atomic coordinates and equivalent isotropic displacement

Table 1. Crystal Data and Refinement Parameters for $\text{Rb}_{10}[\text{Si}_6\text{O}_{17}]$ at 150 K

empirical formula	$\text{Rb}_{10}[\text{Si}_6\text{O}_{17}]$
temperature (K)	150
space group, <i>Z</i>	<i>Pbca</i> (No. 61), 4
radiation, λ (Å)	Mo $\text{K}\alpha$, 0.71073
unit cell parameters:	
<i>a</i> (Å)	12.795(3)
<i>b</i> (Å)	13.595(3)
<i>c</i> (Å)	13.739(3)
<i>V</i> (Å ³)	2389.8(8)
μ (mm ^{−1})	20.656
ρ_{calcd} (g/cm ³)	3.600
R_1/wR_2 , $I > 2\sigma$	0.031/0.066
R_1/wR_2 , all data	0.039/0.069

^a $R_1 = \sum ||F_o| - |F_c|| / \sum |F_o|$; $wR_2 = (\sum [w(F_o^2 - F_c^2)^2] / \sum [w(F_o^2)^2])^{1/2}$ where $w = 1/[\sigma^2 F_o^2 + (0.0319P)^2 + 11.04P]$ and $P = (F_o^2 + 2F_c^2)/3$.

Table 2. Atomic Coordinates ($\times 10^4$) and Equivalent Isotropic Displacement Parameters (Å² $\times 10^3$) for $\text{Rb}_{10}[\text{Si}_6\text{O}_{17}]$ at 150 K

atom	Wyckoff position	<i>x</i>	<i>y</i>	<i>z</i>	<i>U</i> _{eq}
Rb(1)	8c	303(1)	2156(1)	3596(1)	12(1)
Rb(2)	8c	2903(1)	2112(1)	4394(1)	16(1)
Rb(3)	8c	2965(1)	3757(1)	2077(1)	18(1)
Rb(4)	8c	3512(1)	4640(1)	4597(1)	13(1)
Rb(5)	8c	4397(1)	111(1)	2733(1)	18(1)
Si(1)	8c	548(1)	2837(1)	1145(1)	8(1)
Si(2)	8c	829(1)	903(1)	120(1)	9(1)
Si(3)	8c	2180(1)	1307(1)	1840(1)	8(1)
O(1) _{br} ^a	8c	119(2)	1851(2)	489(2)	10(1)
O(2) _t ^b	8c	1123(3)	3601(2)	455(2)	16(1)
O(3) _{br}	8c	1418(2)	2307(2)	1884(2)	10(1)
O(4) _t	8c	1458(2)	33871(2)	4163(2)	14(1)
O(5) _{br}	8c	1544(2)	561(2)	1053(2)	12(1)
O(6) _t	8c	2155(3)	787(2)	2880(2)	17(1)
O(7) _t	8c	3292(2)	1578(2)	1391(2)	18(1)
O(8) _t	8c	4591(2)	3249(2)	3241(2)	14(1)
O(9) _{br}	4a	0	0	0	22(1)

^a Bridging oxygen atom situated between two silicon atoms. ^b Terminal oxygen connected to only one silicon atom.

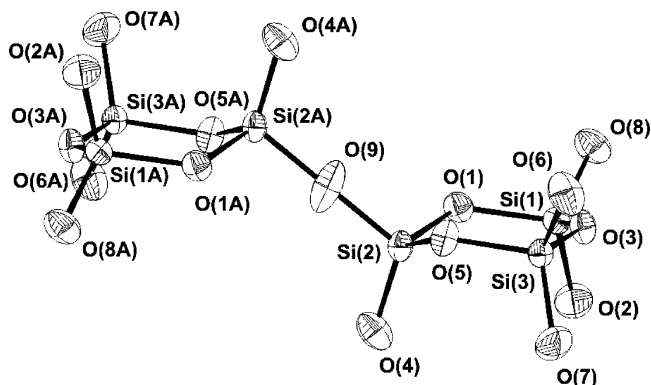


Figure 1. Structure of the novel anion $[\text{Si}_6\text{O}_{17}]^{10-}$ in $\text{Rb}_{10}[\text{Si}_6\text{O}_{17}]$. (Displacement ellipsoids are drawn at the 90% probability level.)

factors are summarized in Table 2. Important Si–O distances are listed in Table 3.

Results

Crystal Structure. The structure of the novel silicate anion $[\text{Si}_6\text{O}_{17}]^{10-}$ is shown in Figures 1 and 2a. The anion consists of six vertex-sharing $[\text{SiO}_4]$ tetrahedra which form two interconnected rings with three tetrahedra in each ring. The lengths of the bridging Si–O bonds (Si–O_{br}) vary between 1.631(1) and 1.705(3) Å, whereas the terminal Si–O (Si–

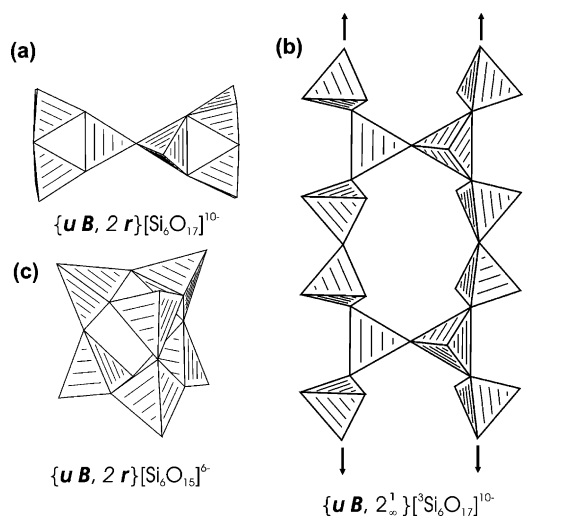
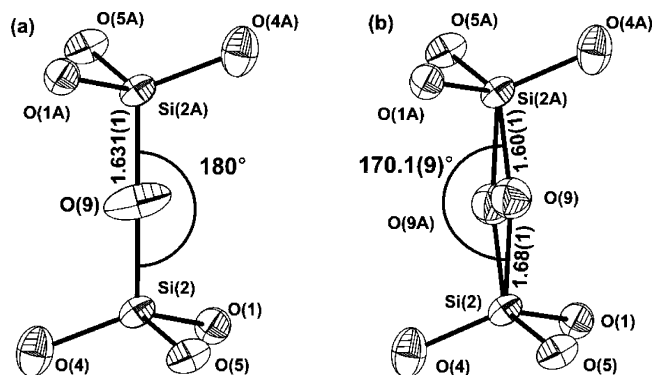
(12) *X-Shape*, v. 1.06; Stoe & Cie: Darmstadt, Germany, 1999; crystal optimization for numerical absorption. *X-RED*, v.1.22; Stoe & Cie: Darmstadt, Germany, 2001; Stoe data reduction program.

(13) (a) Farrugia, L. *J. Appl. Crystallogr.* **1999**, *32*, 837. (b) Sheldrick, G. *Acta Crystallogr., Sect. A* **1990**, *46*, 467. (c) Sheldrick, G. *SHELXL-97*; University of Göttingen: Göttingen, Germany, 1997; a computer program for crystal structure refinement.

Table 3. Si–O Distances at 150 K in $[\text{Si}_6\text{O}_{17}]^{10-}$, Standard Deviation in Units of Last Decimal in Brackets (O_t Denotes Terminal, O_{br} Bridging Oxygen Atoms)

atom–atom contact			atom–atom contact			atom–atom contact		
		<i>d</i> /Å			<i>d</i> /Å			<i>d</i> /Å
Si(1)	–O(8) _t	1.588(3)	Si(2)	–O(4) _t	1.573(3)	Si(3)	–O(7) _t	1.594(3)
	–O(2) _t	1.587(3)		–O(9) _{br}	1.631(1)		–O(6) _t	1.595(3)
	–O(3) _{br}	1.670(3)		–O(5) _{br}	1.642(3)		–O(3) _{br}	1.674(3)
	–O(1) _{br}	1.705(3)		–O(1) _{br}	1.656(3)		–O(5) _{br}	1.692(3)

O_t) bonds are noticeably shorter, with values ranging from 1.573(3) to 1.595(3) Å (Table 3). The shortest Si–O distances are observed at the Si(2) atom, which carries three bridging O atoms. These observations follow the general trends reported previously for silicate structures.¹⁴ The two symmetry-equivalent six-membered rings of the cyclotrisilicate anion are in a flat chair conformation, with a sum of interior angles of 703°. The bridging oxygen atom O(9) is located at a center of symmetry, and consequently, the angle ∠Si(2)–O(9)–Si(2A) is found to be 180° (Figure 3a). However, the elongated displacement ellipsoid, which is almost perpendicular to the Si–O bond (Figure 3a), indicates some disorder of this atomic site (“split position”).

**Figure 2.** Structural motifs of silicate anions with a basic unit consisting of six $[\text{SiO}_4]$ tetrahedra: (a) the anion $[\text{Si}_6\text{O}_{17}]^{10-}$ in $\text{Rb}_{10}[\text{Si}_6\text{O}_{17}]$, (b) the double-chain structure found for the anion in the mineral Xonotlite $\text{Ca}_6[\text{Si}_6\text{O}_{17}](\text{OH})_2$, and (c) the sandwichlike silicate structure in $\text{Na}_3\text{KY}[\text{Si}_6\text{O}_{15}]$.**Figure 3.** Comparison of two structural models for the bridging oxygen atom O(9): (a) linear angle ∠Si–O–Si with O(9) at the crystallographic position (0 0 0) and anisotropic displacement; (b) split positions for O(9) at (0.0063(8) –0.0001(9) –0.0089(7)) at half occupancies and isotropic displacement (both drawn at the 90% probability level). Distances are given in Å.

Thermal Behavior. The composition of the products obtained by heating depends strongly on the reaction temperature. At 400 °C, the starting material SiO_2 as well as RbSi and $\text{Rb}_6[\text{Si}_3\text{O}_9]$ can be detected by powder X-ray diffraction (XRD), whereas at 500 °C, the starting material SiO_2 reacts quantitatively. In all experiments up to 600 °C, $\text{Rb}_6[\text{Si}_3\text{O}_9]$ occurs as the main product, whereas at higher temperatures (700–800 °C), the new compound $\text{Rb}_{10}[\text{Si}_6\text{O}_{17}]$ is formed. Close inspection of the samples showed that at 700 °C two different crystal fractions, a colorless and a red one, have formed. Powder X-ray diffraction measurements of both mechanically separated crystal fractions showed within standard deviations identical lattice parameters, indicating that both fractions were structurally the same. A more detailed analysis of the colorless crystals by means of powder pattern fitting¹⁵ clearly showed that the overall main product $\text{Rb}_{10}[\text{Si}_6\text{O}_{17}]$ was accompanied by some minor amounts of crystalline phases such as α -Si. For details, see the Supporting Information.

The systematic investigation of the composition of the samples at different reaction temperatures indicates that the new silicate $\text{Rb}_{10}[\text{Si}_6\text{O}_{17}]$ evolves from $\text{Rb}_6[\text{Si}_3\text{O}_9]$ initially formed at lower temperatures. This conclusion is supported by differential thermal analysis (DTA) and high-temperature XRD (HT-XRD) experiments of a sample synthesized at 600 °C, which mainly contained $\text{Rb}_6[\text{Si}_3\text{O}_9]$. During the first heating cycle of the sample in a closed Nb crucible, an endothermic effect at 600 °C was observed, followed by an exothermic one at 560 °C upon cooling. A second cycle showed the same behavior of the sample, although with less pronounced effects (for details, see the Supporting Information). Inspection of the products gave evidence for the presence of elemental Rb, and after the removal of the metal by heating in a vacuum, $\text{Rb}_{10}[\text{Si}_6\text{O}_{17}]$ could be identified by its XRD powder pattern.

To establish the solid-to-solid transformation, temperature-dependent XRD experiments were carried out. At lower temperatures up to 400 °C, the weak reflections of RbSi , which was present as a minor phase in the product, disappeared and the lines of the major component $\text{Rb}_6[\text{Si}_3\text{O}_9]$ were shifted to smaller 2θ values still visible up to 750 °C. At 800 °C, new reflections appeared, and the comparison of the data with the calculated powder pattern revealed the formation of $\text{Rb}_{10}[\text{Si}_6\text{O}_{17}]$. Some additional weak new

(14) Smith, J. V.; Bailey, S. W. *Acta Crystallogr.* **1963**, *16*, 801–811.(15) Rodriguez-Carvajal, J. FULLPROF: A program for Rietveld refinement and pattern matching analysis; in *Meeting on Powder Diffraction of the XV Congress of the IUCr*; IUCr: Toulouse, France, 1990; p 127.

reflections could not be indexed, but they might stem from reaction products of rubidium and the quartz glass of the capillary.

IR Spectroscopy. IR spectra (KBr) were recorded before and after the DTA experiments (for the spectra, see the Supporting Information). Three groups of signals could be observed: Between 1200 and 800 cm^{-1} , the Si–O bond stretching modes occurred; the expected signals for cyclic silicates were located in the range between 800 and 600 cm^{-1} ,¹⁶ and in the region below 600 cm^{-1} , the Si–O deformation vibrations were detected.

EPR Spectroscopy. The powder sample of the red fraction of $\text{Rb}_{10}[\text{Si}_6\text{O}_{17}]$ was EPR-inactive in a temperature range between the ambient temperature and the temperature of liquid nitrogen.

Discussion

Structure. The compound $\text{Rb}_{10}[\text{Si}_6\text{O}_{17}]$ contains the novel isolated anion $[\text{Si}_6\text{O}_{17}]^{10-}$ (Figure 2a). The existence of such a dimeric anion (“double-ring”) has been predicted by Liebau, who introduced the general formula $\{\text{uB}, 2r\}[\text{PrSi}_{2p}\text{O}_{6p-l}]^{(4p-2l)-}$ with $p = \text{Pr} \geq 3$ and $1 \leq l \leq p$ for unbranched (uB) double-ring (2r) silicates,^{1,17} and the anion $[\text{Si}_6\text{O}_{17}]^{10-}$ is the first representative of this class of silicates with $p = 3$ and $l = 1$. So far, only double-ring silicates of the formula $\{\text{uB}, 2r\}[\text{PrSi}_{2p}\text{O}_{5p}]^{2p-}$ have been described; an example of which with $p = 3$ is found in the silicate $\text{Na}_3\text{KY}[\text{Si}_6\text{O}_{15}]$ ¹⁸ (Figure 2c). In contrast to the situation in $[\text{Si}_6\text{O}_{17}]^{10-}$ where only one out of three $[\text{SiO}_4]$ tetrahedra within the ring is connected to the second ring, in $[\text{Si}_6\text{O}_{15}]^{6-}$, all tetrahedra are interconnected, thereby forming a sandwichlike structure. An isomeric silicate anion $[\text{Si}_6\text{O}_{17}]^{10-}$ has also been described, which, however, exhibits a completely different arrangement of the six $[\text{SiO}_4]$ tetrahedra. Its structure can be formulated as $\{\text{uB}, 2_{\infty}^1\}[\text{Si}_6\text{O}_{17}]^{10-}$ and displays a one-dimensional, infinite double chain.¹⁹

The unexpected “linear coordination” of the bridging oxygen atom O(9) has been also observed for a large number of silicates, polymorphs of silicon dioxide, and siloxanes and has led to a lively discussion.^{20,21} For the crystallographic treatment of such O atoms, which are located at special crystallographic positions, Liebau suggested a statistical distribution on two symmetrically equivalent sites near the original position, without changing the unit cell or observed crystallographic symmetry.²⁰ Refinement of the O(9) site originally located at the crystallographic position (0, 0, 0) using a “split model” led to the new position [0.0063(8), –0.0001(9), –0.0089(7); $U_{\text{eq}} = 0.0143(12) \text{ \AA}^2$] at a fixed

50% occupation, with a more reasonable angle Si–O–Si of 170.1(7)° and Si–O_{br} distances of 1.60(1) Å and 1.68(1) Å (Figure 3b). This is in good agreement with angles observed for related anions in compounds such as $\text{Cs}_{14}[\text{Si}_4][\text{Si}_6\text{O}_{17}]$ [171(3)°], $\text{Rb}_{14}[\text{Si}_4][\text{Si}_6\text{O}_{17}]$ [168(1)°], and $\text{Rb}_{14}[\text{Ge}_4][\text{Si}_6\text{O}_{17}]$ [165.8(7)°],¹¹ the structure determinations of which did not suffer from “crystallographic restrictions”.

The packing of the $[\text{Si}_6\text{O}_{17}]^{10-}$ anions in the crystals of $\text{Rb}_{10}[\text{Si}_6\text{O}_{17}]$ is in analogy to the arrangement of the S_2 dumbbells in PdS_2 ,²² both dumbbells have a rather similar orientation of their axes with respect to the unit cell edges.

The IR spectra of the silicates $\text{Rb}_6[\text{Si}_3\text{O}_9]$ and $\text{Rb}_{10}[\text{Si}_6\text{O}_{17}]$ show the typical ring-vibration modes between 600 and 800 cm^{-1} .¹⁶ More detailed information especially about the angle $\angle\text{Si}(2)\text{--O}(9)\text{--Si}(2\text{A})$ in $\text{Rb}_{10}[\text{Si}_6\text{O}_{17}]$ would need additional calculations and supporting Raman spectra^{23–26} and are not available yet.

As indicated by the results of the DTA and HT-XRD experiments, the compound $\text{Rb}_{10}[\text{Si}_6\text{O}_{17}]$ seemed to arise from the previously formed cyclotrisilicate $\text{Rb}_6[\text{Si}_3\text{O}_9]$. The fact that, during the HT-XRD experiments, at each investigated temperature, reflections of either $[\text{Si}_6\text{O}_{17}]^{10-}$ or $[\text{Si}_3\text{O}_9]^{6-}$ could be detected suggested that at elevated temperatures solid $\text{Rb}_6[\text{Si}_3\text{O}_9]$ transformed directly to solid $\text{Rb}_{10}[\text{Si}_6\text{O}_{17}]$. Although the isolation of homologous structures with Na, K, or Cs counterions failed up to now, powder diffraction experiments and single-crystal X-ray measurements indicated that a similar condensation also occurred during the formation of $\text{Cs}_{14}[\text{Si}_4][\text{Si}_6\text{O}_{17}]$:²⁷ at lower temperatures, the “silicid silicate” $\text{Cs}_{10}[\text{Si}_4][\text{Si}_3\text{O}_9]$ ¹¹ is formed, which converts upon heating to $\text{Cs}_{14}[\text{Si}_4][\text{Si}_6\text{O}_{17}]$. A similar type of a solid-state condensation was also reported for the potassium silicates $\text{K}_4[\text{SiO}_4]$ and $\text{K}_6[\text{Si}_2\text{O}_7]$,⁵ where at higher temperatures a formal condensation of two isolated $[\text{SiO}_4]^{4-}$ anions led to the formation of the disilicate anion $[\text{Si}_2\text{O}_7]^{6-}$. For the heavier alkaline silicates $\text{A}_6[\text{Si}_2\text{O}_7]/\text{A}_6[\text{Si}_3\text{O}_9]$ ($\text{A} = \text{Rb}$ and Cs),²⁸ the formation of cyclotrisilicate anions from disilicate anions has been observed experimentally. However, in the present case, there are no indications for the appearance of $\text{Rb}_6[\text{Si}_2\text{O}_7]$. It can be assumed that, in analogy to the condensation of OH-containing silicates where H_2O is expelled upon condensation, OH-free alkali-metal silicates may release “ A_2O ” upon the formation of higher aggregates (eq 1).



The release of Rb_2O is difficult to detect, however, because

(16) Matossi, F.; Krüger, H. Z. *Phys.* **1936**, *99*, 1.

(17) Nomenclature according to Liebau: uB, unbranched (branchedness); 2r, two rings (multiplicity and dimensionality); Pr, periodicity; p, number of $[\text{SiO}_4]$ tetrahedra; l, number of linkages between the two rings.

(18) Sokolova, E.; Hawthorne, F. C.; Agakhanov, A. A.; Pautov, L. A. *Can. Mineral.* **2003**, *41*, 513–520.

(19) Mamedov, K. S.; Belov, N. V. *Dokl. Akad. Nauk SSSR* **1956**, *85*, 13–38.

(20) Liebau, F. *Acta Crystallogr.* **1961**, *14*, 1103–1109.

(21) Cruickshank, W. J.; Lynton, H.; Barclay, G. A. *Acta Crystallogr.* **1962**, *491–498*.

(22) Grønvd, F.; Røst, E. *Acta Crystallogr.* **1957**, *10*, 329–331.

(23) Kim, C. C.; Bell, M. I.; McKeown, D. A. *Phys. Rev. B: Condens. Matter Mater. Phys.* **1993**, *48*, 7869–7877.

(24) McKeown, D. A.; Bell, M. I.; Kim, C. C. *Phys. Rev. B: Condens. Matter Mater. Phys.* **1993**, *48*, 16357–16365.

(25) McKeown, D. A.; Nobles, A. C.; Bell, M. I. *Phys. Rev. B: Condens. Matter Mater. Phys.* **1996**, *54*, 291–304.

(26) Gabelica-Robert, M.; Tarte, P. *Spectrochim. Acta, Part A* **1979**, *35*, 649–654.

(27) $\text{Cs}_{14}[\text{Si}_4][\text{Si}_6\text{O}_{17}]$: $M = 2413.64 \text{ g/mol}$; monoclinic; $P2_1/c$ (No. 14); $a = 15.162 \text{ \AA}$, $b = 8.228(3) \text{ \AA}$, $c = 33.945(7) \text{ \AA}$; $\beta = 104.03(3)^\circ$; $V = 2408.5(8) \text{ \AA}^3$; $Z = 4$. In Hoffmann, S. Doctoral Dissertation, ETH Zürich: Zürich, Switzerland, 2003.

the reaction is accompanied by the formation of small amounts of RbSi, elemental Rb, and amorphous components. Thus, a depletive interpretation of the observed thermal effects during the DTA experiment is very delicate. However, the endothermic effect in the range between 600 and 700 °C could be explained by the transformation of $\text{Rb}_6\text{[Si}_3\text{O}_9\text{]}$ to $\text{Rb}_{10}\text{[Si}_6\text{O}_{17}\text{]}$, and the exothermic effect upon cooling might stem from the condensation of rubidium or rubidium oxide.²⁹ The occurrence of the same effects between 600 and 700 °C during the second cycle may indicate an incomplete reaction during the first heating period. The red color observed for some but not all of the samples cannot be explained so far. From the result of CW-EPR spectroscopy, paramagnetic centers do not seem to be responsible for that observation.

In summary, we introduced a new silicate with the novel anion $\text{[Si}_6\text{O}_{17}\text{]}^{10-}$ and suggested that its formation took place via a solid-state condensation reaction of the cyclotrisilicate anion $\text{[Si}_3\text{O}_9\text{]}^{6-}$. The preparation method using a closed niobium ampule and elemental rubidium seemed to enhance

(28) Schartau, W. In *Neue Titanate, Germanate und Silicate der Alkali-metalle*; Universität Giessen: Giessen, Germany, 1974.

(29) Boiling point of rubidium at approximately 690 °C.

the crystallization process of silicates as compared to conventional syntheses starting from Rb_2CO_3 and SiO_2 in an open system, where glass formation is often encountered. Furthermore, the synthesis and structure determination of $\text{Rb}_{10}\text{[Si}_6\text{O}_{17}\text{]}$ shows that the recently reported structures of $\text{Rb}_{14}\text{[Si}_4\text{][Si}_6\text{O}_{17}\text{]}$ and $\text{Rb}_{14}\text{[Ge}_4\text{][Si}_6\text{O}_{17}\text{]}$ are indeed fascinating intergrowth structures of a stable oxide ($\text{Rb}_{10}\text{[Si}_6\text{O}_{17}\text{]}$) and a Zintl phase [$\text{RbSi (Rb}_4\text{Si}_4\text{)}$ and $\text{RbGe (Rb}_4\text{Ge}_4\text{)}$, respectively].

Acknowledgment. We thank Prof. B. Eisenmann and Dr. E. Maverick for the helpful discussion of our results. S. Eck is kindly acknowledged for his help in preparing samples for the IR measurements. Prof. K.-P. Dinse and Dr. P. Jakes are thanked for the recording of EPR spectra. The authors thank Dr. Annette Schier for her help with the correction of the manuscript.

Supporting Information Available: X-ray crystallographic files in CIF format, X-ray powder diffraction pattern of $\text{Rb}_{10}\text{[Si}_6\text{O}_{17}\text{]}$, DTA trace for $\text{Rb}_6\text{[Si}_3\text{O}_9\text{]}$, and IR spectra of $\text{Rb}_6\text{[Si}_3\text{O}_9\text{]}$ and $\text{Rb}_{10}\text{[Si}_6\text{O}_{17}\text{]}$. This material is available free of charge via the Internet at <http://pubs.acs.org>.

IC0610886